Temperature dependence of the photothermal laser cooling efficiency for a micro-cantilever*

Ding Li-Ping(丁丽萍)[a)b)], Mao Tian-Hua(毛添华)[a)b)], Fu Hao(付 号)[a)], and Cao Geng-Yu(曹更玉)[a)†]

[a)] *State Key Laboratory of Magnetic Resonance and Atomic and Molecular Physics, Wuhan Institution of Physics and Mathematics, Chinese Academy of Sciences, Wuhan* 430071, *China*

[b)] *University of Chinese Academy of Sciences, Beijing* 100049, *China*

(Received 4 April 2014; revised manuscript received 30 May 2014; published online 10 August 2014)

The relationship between the photothermal cooling efficiency of a micro-cantilever's mechanical mode and the environmental temperature is studied. The micro-cantilever and a polished fiber end form a low finesse Fabry–Perot (FP) cavity. Experimental results in a temperature range from 77 K to 298 K show that temperature has an obvious influence on photothermal cooling efficiency. The photothermal cooling efficiency, $\eta_{\rm ph}$, at 100 K is 10 times that at 298 K. This accords well with the theoretical analysis that the high photothermal cooling efficiency can be achieved when photothermal response time, $\tau_{\rm ph}$, and mechanical resonant frequency, ω_0, are close to the optimal photothermal cooling condition $\omega_0\tau_{\rm ph}=1$. Our study provides an important approach for high effective photothermal cooling and high-sensitivity measurement for force microscopy.

Keywords: micro-cantilever, FP cavity, photothermal cooling, temperature dependence, optomechanics

PACS: 78.20.nb, 42.60.–v, 42.55.Sa **DOI:** 10.1088/1674-1056/23/10/107801

1. Introduction

Owing to the optomechanical coupling between optical cavity field and mechanical degree of freedom, the laser cooling of mechanical motion of a cantilever can be realized in several ways,[1] such as radiation pressure[2–7] and photothermal cooling.[8–13] Quantum ground state of mesoscopic objects could be prepared by resolved sideband cooling, in which high finesse cavity and high mechanical quality factor are essential for getting a strong coupling of radiation pressure.[3–6] Under the condition of resolved sideband cooling, Kippenberg *et al*. have successfully cooled a mechanical resonator (MR) to the ground state using a radiation pressure mechanism.[7] Photothermal cooling has also attracted much attention in applied optomechanical field because it can be realized in most optical systems with no requirement of ultra-high finesse optical cavity.[10–13] Pioneering theoretical and experimental studies have demonstrated that photothermal cooling of MR possesses high potential applications in high-sensitivity measurements, owing to its strong capacity for suppressing thermal noise.[14–16] Under high vacuum condition at room temperature, Karrai *et al*. have studied photothermal coupling and cooled the gold coated micro-cantilever to 18 K.[12] However, photothermal cooling efficiency is restricted by many factors, such as laser absorption-induced heating, optical bistability, and contribution from higher order mechanical modes.[17–19] Laser absorption-induced heating in the MR is determined by the properties of materials and is difficult to reduce. Our previous work has shown that the restriction on the photothermal cooling efficiency, which is imposed by higher order mechanical modes, can be overcome by operating in the parallel coupling region.[17] However, the optical bistability effect still limits the maximum optical power in photothermal cooling.[18,19] Thus, how to achieve a high efficient photothermal cooling is a critical issue in optomechanics because it can not only reduce the thermal noise but it is also important in increasing the threshold of bistability.

In this paper, we investigate the influence of temperature on the photothermal cooling efficiency of an optomechanical system in a micro-cantilever-based Fabry–Perot (FP) cavity. To search the relationship between the photothermal cooling efficiency and temperature, we use a variable temperature system in which the temperature can vary from 77 K up to 298 K. Through measurements and analyses of the vibration power density spectrum, the photothermal cooling efficiency can be obtained. Furthermore, we analyze the optimal photothermal cooling condition with a theoretical model.

2. Experiment

The experimental setup is shown in Fig. 1. A 300-μm-long, 10-μm-wide, and 0.85-μm-thick single-crystal silicon micro-cantilever coated with 50-nm-thick gold film on both sides, as shown in Fig. 2, was used.[20] Gold coating was used to enhance the photothermal coupling.[21,22] In order to balance the bending of the cantilever caused by the difference in thermal expansion coefficient between two materials, the cantilever was double-side coated. To avoid air viscous

*Project supported by the National Basic Research Program of China (Grant No. 2012CB922101).

†Corresponding author. E-mail: gycao@wipm.ac.cn

© 2014 Chinese Physical Society and IOP Publishing Ltd

damping, a cavity optomechanical system was placed in an ultra-high vacuum chamber with a base pressure better than 5×10^{-10} Torr (1 Torr = 1.33322×10^{2} Pa). Under an ultra-high vacuum condition at room temperature, the intrinsic resonant frequency ω_0 and damping factor Γ_0 of the gold-coated cantilever are $2\pi\times9897.053$ Hz and $2\pi\times4.141$ Hz, respectively. The gold-coated micro-cantilever and a polished fiber end formed a low finesse FP cavity. By measuring the reflected beam from the FP cavity, the finesse of the cavity is estimated to be about 0.6. The distance between the cantilever and fiber end can be adjusted in three dimensions by a PZT positioner. A 1310-nm laser interferometer was used to measure the mechanical motion of the cantilever. An FFT spectrum analyzer (SR760, Stanford Research System) was used to analyze the mechanical dynamics of the cantilever in the frequency domain. During the experiment, the whole cavity optomechanical system was placed in a liquid nitrogen cryostat. A temperature controller (Lakeshore 340) was employed to control an electronic heater to raise the temperature stably from 77 K to 298 K, the precision of the temperature control is about ±0.1 K.

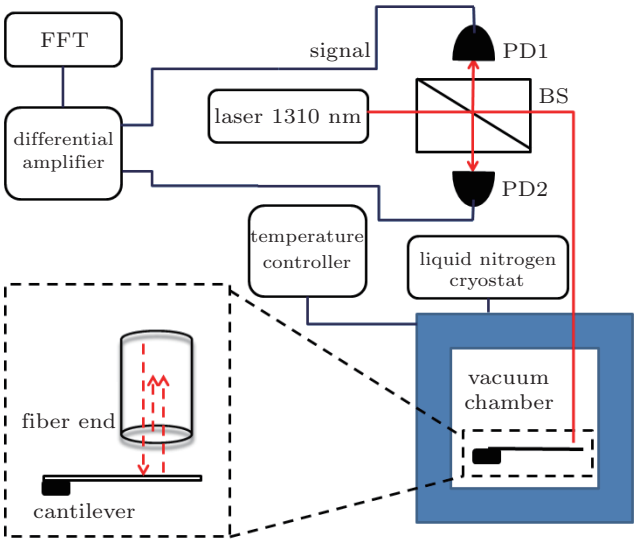


Fig. 1. (color online) Schematic diagram of the experimental setup. A 3-dB optical coupler (Beam Splitter) splits the 1310-nm laser beam into two parts, one is for reference signal and the other is fed into the system which is used for driving the optical cavity and detecting the interference. The fiber end with the cantilever forms a Fabry–Perot cavity, which is placed in an ultrahigh vacuum chamber and then moved into a liquid nitrogen cryostat. Temperature controller can change the temperature steadily from 77 K to 298 K.

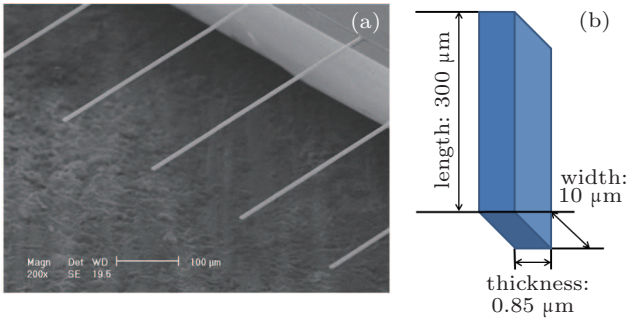


Fig. 2. (color online) (a) SEM image of the single crystal silicon micro-cantilever. (b) Key dimensions of the micro-cantilever: 300-μm long, 10-μm wide, and 0.85-μm thick.

3. Results

To realize photothermal cooling, the FP cavity is set at blue detuning.[12] The vibrations of power spectral density of the cantilever at different laser powers are measured at 77 K and 298 K, respectively, as shown in Fig. 3. The vibration resonance curves are fitted by Lorentz function, in which the peak center and the full width at half maximum (FWHM) represent the effective resonant frequency $\omega_{\rm eff}$ and effective damping factor $\Gamma_{\rm eff}$, respectively. In Fig. 3(a), the Brownian motion of the cantilever is greatly suppressed as the laser power increases at 77 K. But at 298 K the vibration power spectral densities under different laser powers are almost the same as those shown in Fig. 3(b), this suppressing effect is much weaker than at 77 K. Our experimental results show that $\Gamma_{\rm eff}$ increases from $2\pi\times0.524$ Hz to $2\pi\times4.744$ Hz at 77 K as the laser power increases from 132 μW to 2842 μW. However, at 298 K, $\Gamma_{\rm eff}$ changes only from $2\pi\times3.890$ Hz to $2\pi\times4.145$ Hz with laser power increasing from 306 μW to 3771 μW. From the changes of effective damping factor $\Gamma_{\rm eff}$ at 77 K and 298 K, it follows that the photothermal cooling efficiency shows a strong dependence on temperature.

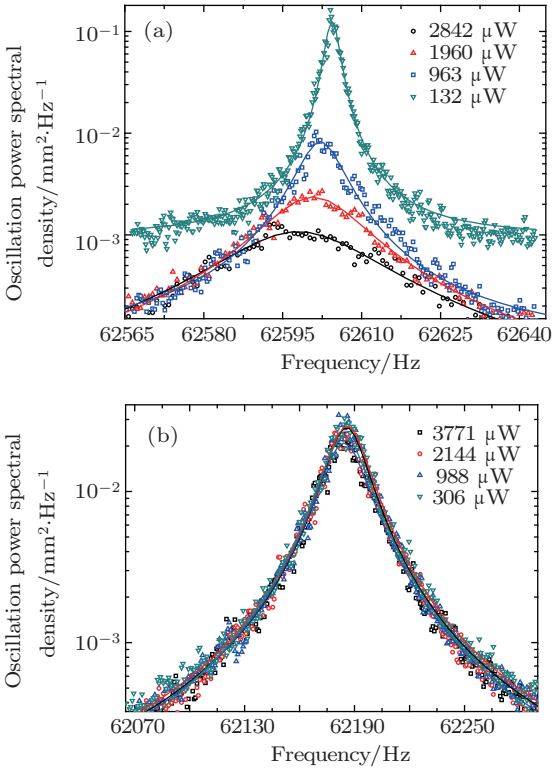


Fig. 3. (color online) Oscillation power spectral densities of the cantilever at 77 K (a) and 298 K (b). All of the vibration resonance curves for different laser powers are fitted to Lorentz function, in which the peak center and the full width at half maximum (FWHM) represent the effective resonant frequency $\omega_{\rm eff}$ and effective damping factor $\Gamma_{\rm eff}$, respectively. The power density spectrum corresponds to the fundamental mechanical mode of the micro-cantilever.

In order to obtain the relationship between photothermal cooling efficiency and temperature, we measure the vibration power spectral density as the temperature changes from 77 K to 298 K. The values of effective damping factor $\Gamma_{\rm eff}$ at different temperatures are plotted against incident laser power in Fig. 4. Although the effective damping factor $\Gamma_{\rm eff}$ shows a linear increase with incident laser power, the increasing rates of $\Gamma_{\rm eff}$ under different temperatures are different. At 77 K and 100 K, the values of effective damping factor $\Gamma_{\rm eff}$ increase much quicker than those at higher temperatures of 160 K, 230 K, and 298 K. From the experimental data, the slope of $\Gamma_{\rm eff}$ increases to a maximum value at 100 K.

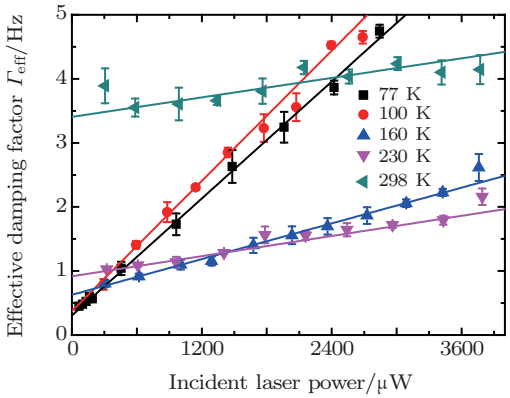


Fig. 4. (color online) Effective damping factors versus incident laser power of the cantilever at temperatures ranging from 77 K to 298 K. The points denote the experimentally measured data, and lines represent their linear fitting.

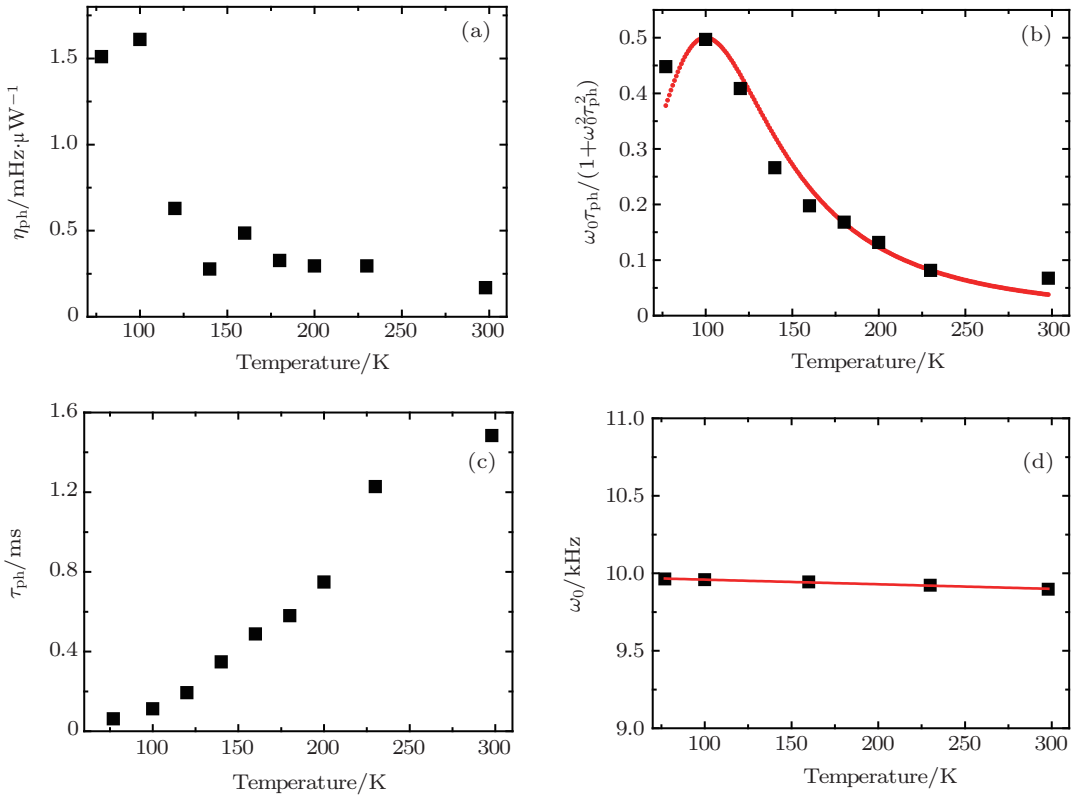


Fig. 5. (color online) Temperature-dependent photothermal cooling efficiency $\eta_{\rm ph}$ (a), simulative value of $\omega_0\tau_{\rm ph}/(1+\omega_{\rm w}^2\tau_{\rm ph}^2)$, with the solid line representing its fitting (b), calculated value of response time constant of photothermal force $\tau_{\rm ph}$ (c), and measured intrinsic resonant frequency ω_0 (d). It is clear that the resonant frequency change is relatively small. The points denote the experimental measurement data, and the solid line represents its linear fitting.

4. Discussion

To further analyze the photothermal cooling efficiency dependence on temperature, a parameter $\eta_{\rm ph} = {\rm d}\Gamma_{\rm eff}/{\rm d}P$ is defined, where P denotes the laser power. The values of $\eta_{\rm ph}$ at different temperatures are plotted in Fig. 5(a). The photothermal cooling efficiency $\eta_{\rm ph}$ shows a nonlinear dependence on temperature in a range from 77 K to 298 K. The photothermal cooling efficiency increases from 77 K to 100 K. At 100 K, it reaches a maximum value of $\eta_{\rm ph} = 1.610$ mHz/μW. With the further increase of temperature, it causes the efficiency to gradually decrease from 100 K to 298 K. When the temperature is close to the room temperature, $\eta_{\rm ph}$ decreases to 0.168 mHz/μW, which is almost ten per cent of that at 100 K.

Previous studies on photothermal cooling have shown that the backaction of photothermal force is not instantaneous but delayed with respect to the mechanical motion of a microcantilever.[23] The response time constant of photothermal force, $\tau_{\rm ph}$, is the time of thermal diffuse along the cantilever.

Thermal diffusion time is determined by many parameters related to temperature, such as material heat capacity, thermal conductivity, and the laser spot position. The laser spot position can be regarded as a fixed value according to our calibrated result that the laser spot position change is only 2.8% from 77 K to 160 K.

From Ref. [24], we can deduce that the relationship between the photothermal cooling efficiency $\eta_{\rm ph}$ and response time constant $\tau_{\rm ph}$ can be described as

$$\eta_{\rm ph} \propto \omega_0 \tau_{\rm ph}/(1+\omega_0^2\tau_{\rm ph}^2).$$

The response time constant of photothermal force $\tau_{\rm ph}$ can be calculated according to Ref. [25], the results are shown in Fig. 5(c). The intrinsic resonant frequency ω_0 changing with temperature is shown in Fig. 5(d). The frequency change is only 0.67% from 77 K to 298 K, thus the resonant frequency change can be omitted in our calculation and ω_0 has been considered to be a constant of $2\pi \times 9897.053$ Hz for different temperatures. The calculated values of $\omega_0\tau_{\rm ph}/(1+\omega_0^2\tau_{\rm ph}^2)$ at different temperatures are plotted in Fig. 5(b). It is quite clear that the theoretical calculation results are in excellent agreement with our experimental data.

To obtain the maximum value of photothermal cooling efficiency $\eta_{\rm ph}$, ω_0 and $\tau_{\rm ph}$ should satisfy the condition of $\omega_0\tau_{\rm ph} = 1$, i.e., $\omega_0\tau_{\rm ph}/(1+\omega_0^2\tau_{\rm ph}^2)$ reaches the maximum value. As shown in Fig. 5(c), the response time constant of photothermal force $\tau_{\rm ph}$ increases as temperature increases. The response time constant $\tau_{\rm ph}$ reaches a value of 1.12 ms at 100 K and $\omega_0\tau_{\rm ph} = 1.11$, which is much closer to the optimal photothermal cooling condition $\omega_0\tau_{\rm ph} = 1$ than at other temperatures. At 298 K the value of $\omega_0\tau_{\rm ph}$ is 14.8, which is far from 1. Therefore, the maximum of photothermal cooling efficiency is achieved at 100 K in our experiment. When the temperature increases above 100 K, $\tau_{\rm ph}$ increases rapidly. Thus the photothermal backaction is averaged over time, which causes the photothermal cooling efficiency $\eta_{\rm ph}$ to decrease from 100 K to 298 K, as shown in Fig. 5(a). Therefore the photothermal cooling efficiency can be optimized by a temperature to meet the optimal photothermal cooling condition, $\omega_0\tau_{\rm ph} = 1$.

At a given temperature, the material properties of the cantilever are determinate, and then the value of $\omega_0\tau_{\rm ph}$ is determined by the cantilever geometry. Thus, through the proper design of the cantilever, the optimal photothermal cooling condition $\omega_0\tau_{\rm ph} = 1$ can also be satisfied. We believe that optimal photothermal cooling condition can also be reached in other photothermal optomechanical systems.

5. Conclusions

We have studied the relationship between photothermal cooling efficiency and temperature in a micro-cantilever-based low finesse FP cavity optomechanical system. Our experimental results show that temperature has a significant influence on the photothermal cooling efficiency, which can be well explained by a relationship between the cooling efficiency $\eta_{\rm ph}$ and response time $\tau_{\rm ph}$. In our case, the maximum photothermal cooling efficiency $\eta_{\rm ph}$ is obtained at 100 K, when the optimal photothermal cooling condition $\omega_0\tau_{\rm ph} = 1$ is satisfied. We conclude that the photothermal cooling efficiency can be improved, with the optimal condition $\omega_0\tau_{\rm ph} = 1$ satisfied, through the proper design and fabrication of the mechanical resonator. This approach supplies an important way to improve photothermal cooling efficiency, which could be used in high-sensitivity measurements.

References

[1] Liu Y C, Hu Y W, Wong C W and Xiao Y F 2013 *Chin. Phys. B* **22** 114213

[2] Arcizet O, Cohadon P F, Briant T, Pinard M and Heidmann A 2006 *Nature* **444** 71

[3] Dantan A, Genes C, Vitali D and Pinard M 2008 *Phys. Rev. A* **77** 011804

[4] Gigan S, Böhm H R, Paternostro M, Blaser F, Langer G, Hertzberg J B, Schwab K C, Bäuerle D, Aspelmeyer M and Zeilinger A 2006 *Nature* **444** 67

[5] Corbitt T, Ottaway D, Innerhofer E, Pelc J and Mavalvala N 2006 *Phys. Rev. A* **74** 021802

[6] Chen H J and Mi X W 2011 *Chin. Phys. B* **20** 124203

[7] Schliesser A, Del'Haye P, Nooshi N, Vahala K J and Kippenberg T J 2006 *Phys. Rev. Lett.* **97** 243905

[8] Jourdan G, Comin F and Chevrier J 2008 *Phys. Rev. Lett.* **101** 133904

[9] Metzger C H, Ludwig M, Neuenhahn C, Ortlieb A, Favero I, Karrai K and Marquardt F 2008 *Phys. Rev. Lett.* **101** 133903

[10] Fu H, Liu Y, Chen J and Cao G Y 2010 *Sens. Actuators A* **163** 533

[11] Barton R A, Storch I R, Adiga V P, Sakakibara R, Cipriany B R, Ilic B, Wang S P, Peijie Ong, McEuen P L, Parpia J M and Craighead H G 2012 *Nano Lett.* **12** 4681

[12] Metzger C H and Karrai K 2004 *Nature* **432** 1002

[13] Liberato S D, Lambert N and Nori F 2011 *Phys. Rev. A* **83** 033809

[14] Dang H B, Maloof A C and Romalis M V 2010 *Appl. Phys. Lett.* **97** 151110

[15] Schliesser A, Arcizet O, Rivi'ere R, Anetsberger G and Kippenberg T J 2009 *Nat. Phys.* **5** 509

[16] Sadewasser S, Jelinek P, Fang C K, Custance O, Yamada Y, Sugimoto Y, Abe M and Morita S 2009 *Phys. Rev. Lett.* **103** 266103

[17] Fu H, Liu C D, Liu Y, Chu J R and Cao G Y 2012 *Opt. Lett.* **37** 584

[18] Vogel M, Mooser C and Karrai K 2003 *Appl. Phys. Lett.* **83** 1337

[19] Venstra W J, Westra H J R and van der Zant H S J 2010 *Appl. Phys. Lett.* **97** 193107

[20] Liu Y, Kong W, Zhang T L, Zhao G and Chu J R 2010 *5th IEEE International Conference on Nano/Micro Engineered and Molecular Systems*, January 20–23, Xiamen, China, p. 633

[21] Datskos P G and Sauers I 1999 *Sens. Actuators B: Chemical* **61** 75

[22] Serrano J R, Phinneya L M and Rogers J W 2009 *Int. J. Heat Mass Transfer* **52** 2255

[23] Abdi M and Bahrampour A R 2012 *Phys. Rev. A* **85** 063839

[24] Metzger C H, Favero I, Ortlieb A and Karrai K 2008 *Phys. Rev. B* **78** 035309

[25] Barnes J R, Stephenson R J, Woodburn C N, O'Shea S J, Welland M E, Rayment T, Gimzewski J K and Gerber Ch 1994 *Rev. Sci. Instrum.* **65** 3793